Published for SISSA by Springer

Received: *February 4, 2016*
Accepted: *May 17, 2016*
Published: *June 6, 2016*

The fate of the Higgs vacuum

Philipp Burda,[a,b,1] **Ruth Gregory**[b,c] **and Ian G. Moss**[d]

[a] *Racah Institute of Physics, Hebrew University, Jerusalem 91904, Israel*
[b] *Centre for Particle Theory, Durham University, South Road, Durham, DH1 3LE, U.K.*
[c] *Perimeter Institute, 31 Caroline Street North, Waterloo, ON, N2L 2Y5, Canada*
[d] *School of Mathematics and Statistics, Newcastle University, Newcastle Upon Tyne, NE1 7RU, U.K.*

E-mail: philipp.burda@mail.huji.ac.il, r.a.w.gregory@durham.ac.uk, ian.moss@newcastle.ac.uk

Abstract: We have recently suggested that tiny black holes can act as nucleation seeds for the decay of the metastable Higgs vacuum. Previous results applied only to the nucleation of thin-wall bubbles, and covered a very small region of parameter space. This paper considers bubbles of arbitrary profile and reaches the same conclusion: black holes seed rapid vacuum decay. Seeded and unseeded nucleation rates are compared, and the gravitational back reaction of the bubbles is taken into account. The evolution of the bubble interior is described for the unseeded nucleation. Results are presented for the renormalisation group improved Standard Model Higgs potential, and a simple effective model representing new physics.

Keywords: Black Holes, Nonperturbative Effects, Solitons Monopoles and Instantons

ArXiv ePrint: 1601.02152

[1] On leave of absence from ITEP, Moscow.

doi:10.1007/JHEP06(2016)025

Contents

JHEP06(2016)025

1 Introduction

Although many phase transitions in physical models are second order, our intuitive picture of a phase transition is determined by our most common experience: boiling water. Such a first order phase transition proceeds by nucleation of bubbles of the new phase, often around impurities, which then expand. This intuitive picture of a first order phase transition has a corresponding physical and mathematical analogy in quantum phase transitions between different vacua [1–4]. Such decay processes have current relevance due to the possible metastability of the Higgs vacuum [5–10], mooted some time ago [11–19], but lent recent credence by the measured value of the Higgs mass [20, 21].

The nucleation of a bubble of a different vacuum phase was described in a series of papers by Coleman and collaborators [1–3], in which a Euclidean approach is used to describe the leading order contribution to the wavefunction for decay. For vacua separated by large barriers, this is well approximated by assuming the two vacua are separated by relatively thin wall of energy, throughout which the fields vary from one vacuum to the other. The gravitational effect of this "thin-wall", as well as of the corresponding vacuum energies, can be computed precisely in (Euclidean) Einstein gravity [22], using the Israel equations [23] to model the bubble wall. Coleman and de Luccia [3] described this physical picture of vacuum decay in the universe, and presented the Coleman-de Luccia (CDL) instanton, which is now the "gold standard" for describing vacuum decay.

The single instanton picture of Coleman et al. is however extremely idealised. There are no features to the solution other than the bubble — in particular, no description of inhomogeneities. Given the gravitational set-up of CDL, the most natural and simplest inhomogeneity to introduce is a black hole, and although early work did explore this [24–26], it failed to properly account for the impact of the conical deficits that inevitably arise in the

Euclidean calculations. In [27], the effect of said conical deficits was carefully computed, and a potentially large enhancement of the CDL rates was demonstrated in the context of tunnelling from a positive to zero cosmological constant. (See also [28] for a study of general thin wall solutions.)

Applying these ideas to the Higgs vacuum, in [29, 30] we recently provided a proof of principle that the lifetime of the vacuum could become precipitously short in the presence of primordial black holes, paralleling the intuition of impurities catalysing a phase transition. However, the semi-analytic arguments we used (based on the Israel "thin-wall" formalism [23]) meant that we could only apply these conclusions to a very small and artificial region of parameter space within a (quantum gravity) corrected Higgs potential. In [29], we provided preliminary evidence that this parameter space restriction was an artefact of the constraints imposed on the potential by demanding that it allow a thin-wall approximation for the instanton. The purpose of this paper is to confirm and flesh out this claim: specifically, by integrating out the coupled Einstein-Higgs equations of motion for a Euclidean instanton solution, we will show that for a wide range of BSM / quantum gravity corrections (or indeed none at all!) to the Higgs potential, the presence of a micro-black hole can prove lethal to our universe.

2 "Standard" Higgs vacuum decay

Before embarking our presentation, we first briefly review the standard description of vacuum decay. We discuss the simplified parametrisation of the Higgs potential we will be using in our integrations, then discuss briefly the usual CDL-type instanton, however, rather than approximate this by the Israel-thin-wall description (followed by CDL), we compute this instanton numerically. This generalises previous results on the instanton solutions in flat space [31, 32] and semi-analytical results in de Sitter space [34].

2.1 The Higgs potential

The precise high energy effective potential for the Higgs field has been determined by a two-loop calculation in the context of the standard model [5, 33, 35, 36]. It is conventionally written in terms of an effective coupling, as

$$V(\phi) = \frac{1}{4}\lambda_{\rm eff}(\phi)\phi^4. \tag{2.1}$$

The main uncertainty in the potential is due to the uncertainty of the top quark mass. The potential has a fairly smooth shape which can be computed by direct numerical integration of the $\beta-$functions [17]. Since we are interested in scanning through a range of potentials, and exploring the impact of BSM and quantum gravity corrections, it is expedient to model the potential analytically by fitting to simple functions with a small number of parameters. Although two-parameter fits have been used before [5, 29, 30], we use here a three parameter model,

$$\lambda_{\rm eff}(\phi) = \lambda_* + b\left(\ln\frac{\phi}{M_p}\right)^2 + c\left(\ln\frac{\phi}{M_p}\right)^4. \tag{2.2}$$

JHEP06(2016)025

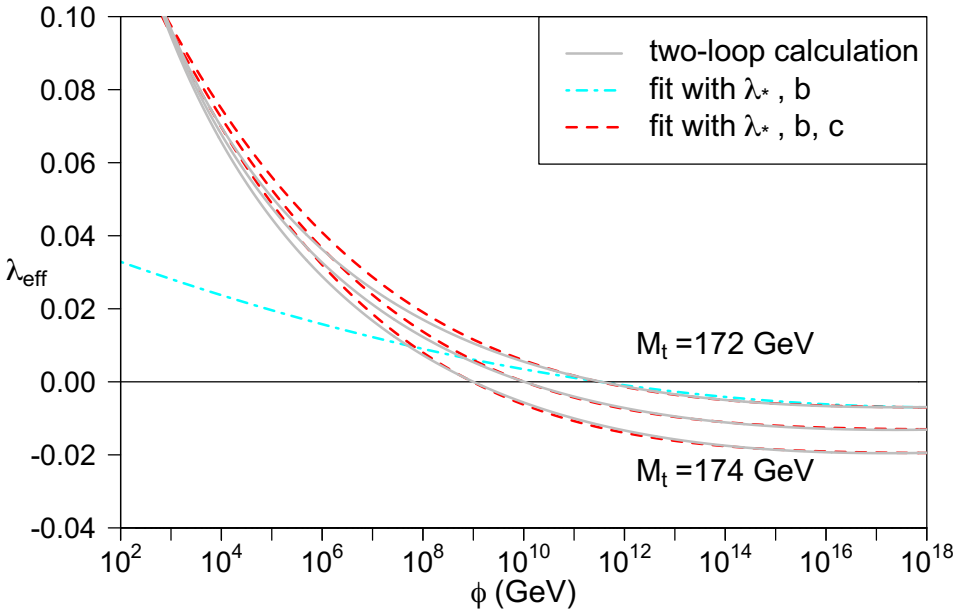

Figure 1. The simplified model of the high-energy effective coupling used for vacuum decay results. The effective coupling has two free parameters when it is fixed at the lower end of the energy range. All three parameters can be fixed by matching to the Standard Model calculation for a given Higgs and top quark mass. The plots show Higgs mass $M_{\rm H} = 125$GeV and top quark masses 172GeV ($\lambda_* = -0.007$), 173GeV ($\lambda_* = -0.013$) and 174GeV ($\lambda_* = -0.00195$). A two parameter model used in earlier work is shown for comparison.

which gives a much better fit over the range of (large) values of ϕ that are relevant for tunnelling phenomena. (See figure 1.)

Since the value of $\lambda_{\rm eff}$ at energies around the Higgs mass is accessible to experimental particle physics, we can fix $\lambda_{\rm eff}$ at the lower end of the range with some confidence. This leaves two fitting parameters, λ_* and b. We shall explore the dependence of our results on both of these parameters, thus our conclusions can be incorporated into more general potentials, including non gravitational BSM corrections.

At very high energies, apart from BSM physics, we may have to contend with the effects of quantum gravity. We adopt the 'effective field theory' approach, and add extra polynomial terms to the potential which contain the mass scale of new physics, in this case the Planck mass [37–39]

$$V(\phi) = \frac{1}{4}\lambda_{\rm eff}(\phi)\phi^4 + \frac{1}{6}\lambda_6\frac{\phi^6}{M_p^2} + \dots \tag{2.3}$$

Adding extra terms to the potential can alter the relationship between the original parameters in $\lambda_{\rm eff}$ and the particle masses. This is one reason why we will give results in terms of the parameters such as λ_*, rather than top quark or other particle masses. It is also easier to see how sensitive (or robust) our conclusions are to the shape of the potential.

JHEP06(2016)025

2.2 The "CDL" instanton

Although Coleman and de Luccia concentrated on the gravitational instanton representing a bubble with an infinitesimally thin domain wall, the CDL instanton is also a good approximation to a wall of finite thickness, as the Israel equations are simply a leading order approximation for a thin, but finite thickness, wall [40, 41]. As we alter the parameters in the potential, the wall can become very thick, to the extent that the Higgs may not even reach the true vacuum in the bubble interior. The key feature of the CDL instanton is however the O(4) symmetry, therefore we refer to an O(4) symmetric configuration of the Einstein-Higgs system that has a bubble of lower vacuum energy inside an asymptotically flat spacetime as a "CDL" instanton, whether it be a 'thin' wall or not.

To find the instanton it is sufficient to consider only a single real component of the Higgs field that we denote by ϕ. The bubble nucleation rate is determined by a bounce solution with Euclidean metric signature $(++++)$, and action

$$S_E = -\frac{1}{16\pi G}\int_{\mathcal{M}} \mathcal{R} + \int_{\mathcal{M}} \left(\frac{1}{2}g^{ab}\partial_a\phi\partial_b\phi + V\right). \tag{2.4}$$

The spacetime geometry should be asymptotically flat with the Higgs field at the false vacuum value, and we take the metric ansatz

$$ds^2 = d\rho^2 + a(\rho)^2\left[d\chi^2 + \sin^2\chi\left(d\theta^2 + \sin^2\theta d\varphi^2\right)\right]. \tag{2.5}$$

The bounce solution $a_b(\rho)$ and $\phi_b(\rho)$ is obtained by solving the Einstein-scalar equations,

$$\phi'' + \frac{3a'}{a}\phi' - \frac{dV}{d\phi} = 0, \tag{2.6}$$

$$(a')^2 = 1 + \frac{8\pi G a^2}{3}\left(\frac{1}{2}(\phi')^2 - V\right). \tag{2.7}$$

The tunnelling exponent is given by the difference in action between the bounce solution and the false vacuum. In this case the false vacuum has zero action, and the tunnelling exponent is simply $B = S_E[a_b, \phi_b]$.

The tunnelling process is a very high energy phenomenon governed by the effective Higgs potential (2.2) with the false vacuum at $\phi = 0$. Requiring solutions which are regular at the origin $\rho = 0$ places additional conditions on the fields,

$$\begin{aligned} &\phi'(0) = 0\,, \quad a'(0) = 1\,, \quad &&\text{at } \rho = 0, \\ &\phi \to 0\,, \qquad a(\rho) \sim \rho\,, \quad &&\text{as } \rho \to \infty. \end{aligned} \tag{2.8}$$

(In ref. [30] we demonstrated that the condition of metric regularity could be loosened to allow conical singularities, but the resulting tunnelling rate was unaffected.)

Solutions were obtained using a shooting procedure, choosing values of ϕ at the origin and integrating outwards to find a solution satisfying the boundary conditions as $\rho \to \infty$. In practice, the boundary conditions are applied at some chosen radius $\rho_{\max}$, and care has to be taken to ensure that the solutions are robust to changes in $\rho_{\max}$ and $\phi(\rho_{\max})$.

JHEP06(2016)025

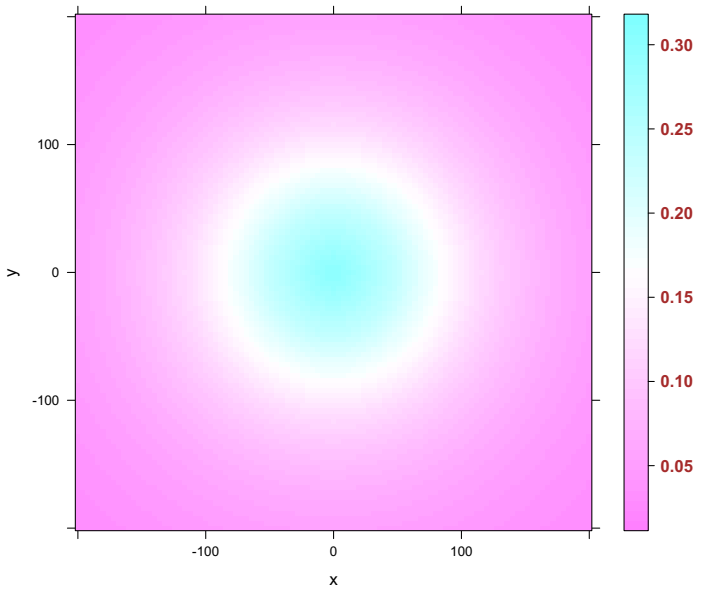

Figure 2. The spatial distribution of the Higgs field in a standard O(4) vacuum decay bubble. Two dimensions are shown, the bounce solution has the same profile in all four dimensions (three space and one imaginary time). The central region of the bubble has large values of ϕ stretching well beyond the potential barrier from the false vacuum (pink) into a new Higgs phase (blue). All measurements are in reduced Planck units. The effective coupling here is modelled by $\lambda_* = -0.01$, $b = 1.4 \times 10^{-5}$, $c = 6.3 \times 10^{-8}$, $\lambda_6 = 0$, corresponding to top quark mass $M_t = 173\text{GeV}$.

An example of the Higgs field for a solution to the Einstein-scalar equation without any QG or BSM corrections is shown in figure 2. The centre of the bounce solution has negative vacuum energy, and the spacetime geometry around $\rho = 0$ has negative curvature. The action of the bounce solution is plotted for a range of Higgs potentials in figure 3. The most important dependence is on the parameter λ_*, which varies with the value of the top quark mass. There is very little dependence on the b parameter.

Recall that the tunnelling rate per unit volume is given by $\Gamma_D = Ae^{-B}$. In the case where the action includes quantum corrections, the pre-factor is determined by the four zero modes which correspond to translations of the O(4) symmetric bounce solution. The zero modes contribute $(B/2\pi)^2$ to the pre-factor A, and there is also a correction from removing the zero modes from the effective action. This part is more difficult to calculate, but dimensional analysis gives a rough estimate r_b^{-4}, where r_b is a characteristic length scale of the bounce solution. For example, the bounce solution in figure 2 has $r_b \sim 100 M_p^{-1}$. To estimate the probability P_D of vacuum decay in the lifetime of the universe, we multiply by the volume and age of the observable universe. We take the size of the universe to be around $10^{61} M_p^{-1}$, leading to $P_D \sim \exp(540 + 2\ln B - B)$, which is comfortably small for the range of B values shown in figure 3.

Now we turn to the effect of physics beyond the standard model, as represented by the ϕ^6 term in the Higgs potential. Positive values of the coefficient λ_6 increase the height of the potential barrier and therefore we expect that this should decrease the vacuum decay rate. On the other hand, as noted in refs. [31, 32], negative values of λ_6 should destabilise the false vacuum.

JHEP06(2016)025

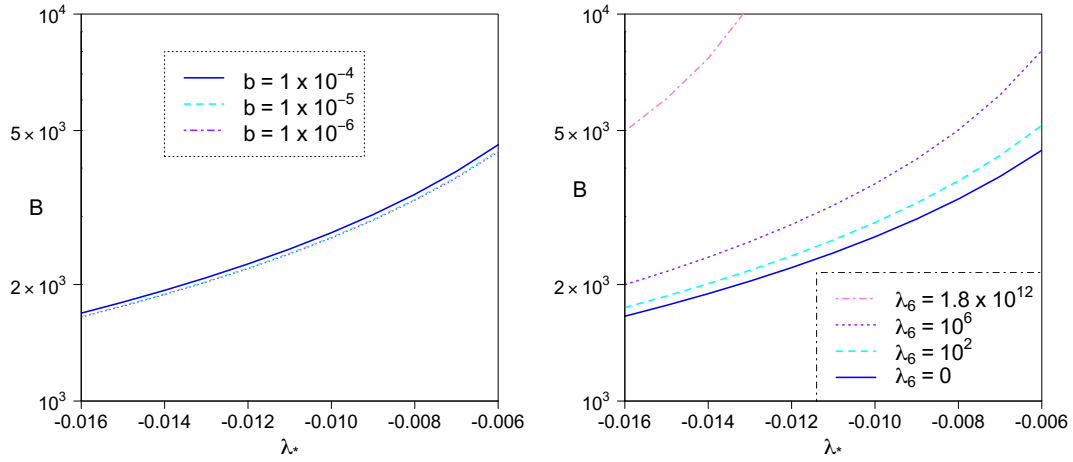

Figure 3. The O(4) bounce action B is shown for a variety of Higgs potentials. The left panel shows results for $\lambda_6 = 0$. The principal dependence is then on the parameter λ_*, which determines the large field limit of the coupling. There is a very weak dependence on the parameter b as shown. The right panel shows the action B as a function of λ_* with $b = 1.4 \times 10^{-5}$, and different values of λ_6.

The bounce action for the O(4) symmetric bounce solution with a range of values for λ_6 is shown in figure 3. As expected, positive values of λ_6 increase the action and reduce the vacuum decay rate. Negative values of λ_6 raise the value of ϕ at the centre of the bubble to be above the Planck scale M_p. The justification for using the effective field theory fails, and we cannot confirm enhancement of the tunnelling rate with the potential and top quark mass ranges we are considering here.

2.3 Bubble evolution in real time

The maximal slice of the bounce solution at $\chi = \pi/2$ represents a bubble which nucleates at an instant of real time. In the thin-wall case, the bubble interior is in the true vacuum, but this is not true for the thick-wall case. In this section we follow the evolution of the interior towards a final state, and see what effect this has on the spacetime geometry.

Following Coleman and De Luccia [3], we perform an analytic continuation of the bounce solution to Lorentzian spacetime. The analytic continuation has to be done carefully because, first of all, the metric is given by a numerical solution and secondly because of the coordinate singularity at $\rho = 0$. To derive the full bubble interior, we start by choosing a more convenient coordinate system (τ, r) instead of (ρ, χ),

$$\tau = f(\rho) \cos \chi, \tag{2.9}$$

$$r = f(\rho) \sin \chi. \tag{2.10}$$

If we choose $f(\rho)$ to satisfy the equation $f' = f/a$, with $f(0) = 0$ and $f'(0) > 0$, then the metric (2.5) becomes conformally flat,

$$ds^2 = \frac{a^2}{f^2} \left(d\tau^2 + dr^2 + r^2 (d\theta^2 + \sin^2 \theta d\varphi^2) \right). \tag{2.11}$$

JHEP06(2016)025

This metric has a very simple analytic continuation to a Lorentzian metric with time coordinate $t = -i\tau$,

$$ds^2 = \frac{a^2}{f^2}\left(-dt^2 + dr^2 + r^2(d\theta^2 + \sin^2\theta d\varphi^2)\right). \tag{2.12}$$

The slice of the bounce solution representing the bubble nucleation which was at $\chi = \pi/2$ is now at $t = 0$. The same analytic continuation of the metric can be applied to the original (ρ, χ) coordinates by taking

$$t = f(\rho)\sinh\psi_+, \tag{2.13}$$

$$r = f(\rho)\cosh\psi_+, \tag{2.14}$$

where $\psi_+ = -i(\pi/2 - \chi)$. These relations show that the coordinate transformation is only valid for the region $r > t$, covering the exterior of the light-cone centred on the point at the middle of the bubble. Since ρ is unaffected by the analytic continuation, the Euclidean bounce solution $\phi_b(\rho)$ becomes an expanding bubble solution $\phi(r,t) = \phi_b(\rho)$. Eqs. (2.13) and (2.14) imply

$$\rho = f^{-1}\left[(r^2 - t^2)^{1/2}\right]. \tag{2.15}$$

Note that, provided $a(\rho) > 0$, then $f(\rho)$ is a monotonic function on the positive real numbers and the inverse f^{-1} exists. The symmetry under Lorentz boosts in r and t is evident. This is the boost part of the full $O(3,1)$ symmetry.

The coordinate system extends trivially through the light cone at $r = t$ and fixes a set of initial conditions at $\rho = 0$ for the evolution of the interior solution,

$$\phi(0) = \phi_b(0), \qquad \phi'(0) = 0. \tag{2.16}$$

In the interior $r < t$, we can define a new coordinate system (ρ_-, ψ_-) which respects the $O(3,1)$ symmetry of the metric,

$$t = f(\rho_-)\cosh\psi_-, \tag{2.17}$$

$$r = f(\rho_-)\sinh\psi_-. \tag{2.18}$$

Again $f' = f/a$, and the interior metric becomes

$$ds^2 = -d\rho_-^2 + a(\rho_-)^2\left(d\psi_-^2 + \sinh^2\psi_-\left(d\theta^2 + \sin^2\theta d\varphi^2\right)\right). \tag{2.19}$$

The Lorentz symmetry preserves spatial hypersurfaces $\rho_- = \text{const}$, and the interior metric in the $O(3,1)$ coordinates is a Friedman metric. The evolution equations are now Lorentzian versions of (2.6), (2.7), with initial conditions set on the light cone by eq. (2.16). An interior solution is shown in figures 4 and 5. Unsurprisingly, since the potential in this example reaches large negative values, the $\phi-$field rolls logarithmically to large values and the 'AdS' spacetime develops a crunch singularity. We see this in figure 4 as a maximum value of $\rho_- = \rho_s$ where $a(\rho_s) = 0$ and the kinetic energy of the scalar field diverges. For $\lambda_6 = 0$, the leading order behaviour of the solutions when $\rho \approx \rho_s$ can be determined analytically, $a \propto (\rho_s - \rho)^{\sqrt{6}/9}$ and $\phi' \propto (\rho_s - \rho)^{-1}$.

JHEP06(2016)025

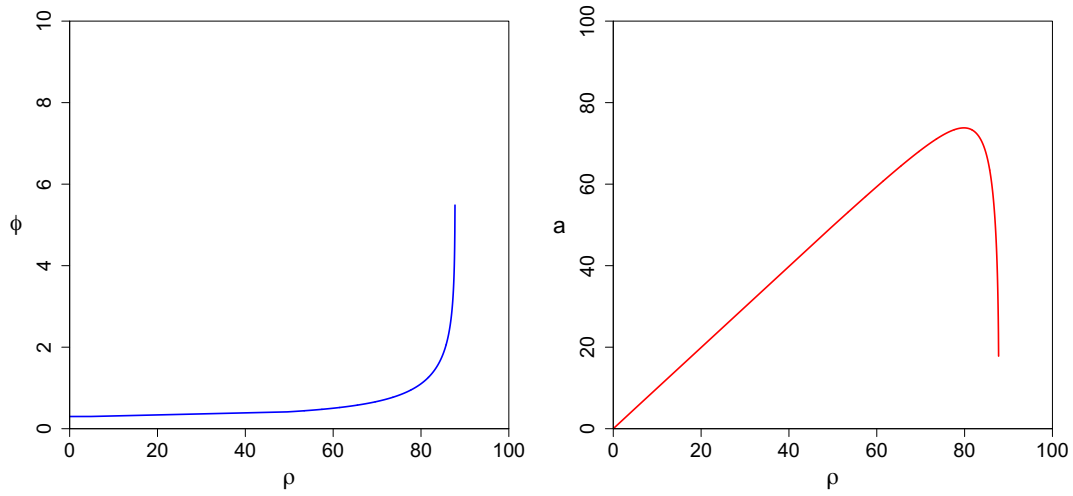

Figure 4. The real-time evolution of the field ϕ and the scale factor a inside the bubble solution shown in figure 2 (which has $\lambda_6 = 0$).

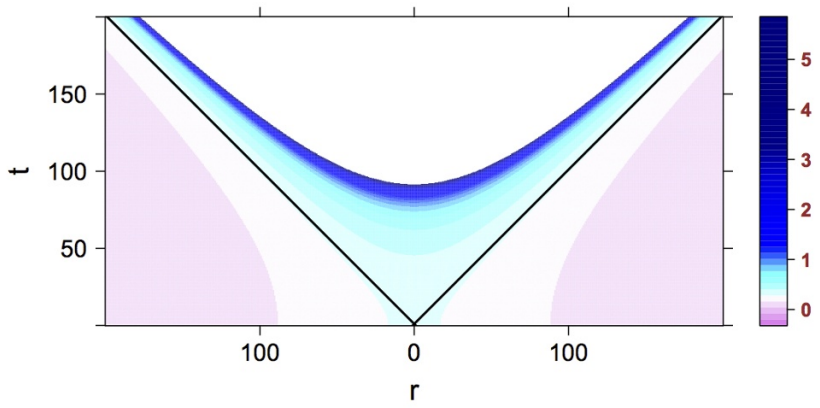

Figure 5. The real-time evolution of the bubble shown in figure 2 using the conformally flat coordinate system. The lightcone centred on the bubble is indicated in black.

3 Vacuum decay seeded by black holes

The main aim of this paper is to obtain instanton solutions in the presence of black holes for general Higgs potentials where the conditions for the thin wall approximation break down. We therefore have to solve the fully coupled Euclidean Einstein-Higgs equations in the presence of a black hole.

First, it will be useful to recall the main conclusions drawn from the thin-wall approximation calculations described in [29, 30]. There, gravitational instantons were constructed with a false vacuum Schwarzschild exterior matched across a domain wall to an exact true vacuum AdS (or Schwarzschild-AdS) interior. These Euclidean solutions exist in principle with all possible values of interior and exterior mass terms, however, for each seed (exterior) mass black hole, there exists a unique least action instanton with a unique remnant (interior) black hole mass. The CDL instanton is a special case where both seed and

JHEP06(2016)025

remnant black hole mass vanish. For very small seed masses, there are instanton solutions that remove the black hole, and the solution has the form of a perturbed CDL instanton. For larger black hole seeds (beyond a critical mass M_C depending on the vacuum energy and the surface tension of the wall) the remnant mass is non-zero and the minimum action solution becomes static in the complex time coordinate.

In earlier sections we adopted the CDL interpretation of the $O(4)$ instanton, taking the solution on a time-symmetric slice to represent the nucleation of a bubble at an instant in real cosmological time. Following this interpretation, black hole instantons represent vacuum decay processes nucleated by black hole seeds, leaving behind black hole remnants when the seed mass exceeds the critical mass M_C. The vacuum decay rate is $\propto e^{-B}$, where B is difference in action between the instanton with a true vacuum bubble and one with the Higgs field entirely in the false vacuum.

The black hole and CDL instantons, like any solution that is periodic in imaginary time, can have a thermal interpretation. In [29, 30], we found that the tunnelling exponent did not depend on the periodicity of the Euclidean time, in other words, on the value of the temperature. In black hole seeded decay, the seed black hole is not thermal, but instead radiating into the surrounding vacuum, with different temperature spectra for the outgoing and ingoing modes. Thus the instanton can only be used in an adiabatic sense, when the evaporation rate of the black hole is negligible compared to the tunnelling rate. This was examined in [29, 30], were we gave a thorough analysis of when the Hawking radiation could be neglected.

As an aside, the CDL instanton itself also has thermal and non-thermal applications in the tunnelling interpretation adopted by Brown and Weinberg [42]. However, the interpretation of the tunnelling instanton used by Brown and Weinberg is not the same as the original interpretation due to CDL that we use here. In particular, their conclusion that static instantons imply thermal tunnelling does not apply in the CDL interpretation.

Returning to the lessons learned from the thin wall case, for seed masses larger than the Planck mass, 10^{-5}g, where the semi-classical approximation can be trusted, we expect to be in the régime dominated by the static instanton. Our strategy therefore is to numerically construct static bounce solutions in the expectation that they will dominate the vacuum decay rate. Even if these solutions do not have the lowest action, this would only mean the static instantons constructed would give an upper bound on the seeded nucleation rate, and our main point about enhancement of the decay rate is made a fortiori.

3.1 Instanton solutions

To construct the instanton, we require a geometry with SO(3) invariance and a Schwarzschild-like mass term; our geometry and scalar field therefore depends on a single radial coordinate r. It proves numerically convenient to take the area gauge, and to parametrise the static, spherically symmetric Euclidean metric as:

$$ds^2 = f(r)e^{2\delta(r)}d\tau^2 + \frac{dr^2}{f(r)} + r^2(d\theta^2 + \sin^2\theta d\varphi^2), \tag{3.1}$$

JHEP06(2016)025

where we write f in the form

$$f = 1 - \frac{2G\mu(r)}{r}. \tag{3.2}$$

The equations of motion for the bounce solution are therefore

$$f\phi'' + f'\phi' + \frac{2}{r}f\phi' + \delta' f\phi' - V_\phi = 0, \tag{3.3}$$

$$\mu' = 4\pi r^2 \left(\frac{1}{2}f\phi'^2 + V\right), \tag{3.4}$$

$$\delta' = 4\pi G r \phi'^2. \tag{3.5}$$

Note that by using (3.5) in (3.3), we can decouple the equations for μ and ϕ, solve, then infer δ by integration of (3.5).

The black hole horizon is defined as usual by the condition $f(r_h) = 0$. It will be convenient to discuss the solutions in terms of a remnant mass parameter $\mu_- = \mu(r_h)$, rather the actual remnant black hole mass, as in the vicinity of the horizon we will typically not be in the true AdS vacuum (our Higgs may not have fallen to its minimum) nor will our horizon radius be expressible as a simple ratio of M_-. Instead, $r_h = 2G\mu_-$ is now a simple ratio of μ_-, and the expressions in our calculations are much clearer. The seed mass M_+ on the other hand is straightforwardly defined as the mass at spatial infinity $r \to \infty$, where the field is in the false vacuum. Finally, since we integrate out from the event horizon, it proves convenient to fix the time co-ordinate gauge there, rather than at asymptotic infinity. This means the $t-$coordinate is no longer the time for an asymptotic observer, however, the action we compute is gauge invariant, hence this is irrelevant.

The boundary conditions are therefore

$$\mu(r_h) = \mu_-, \quad \delta(r_h) = 0, \quad \text{at } r = r_h, \tag{3.6}$$

$$\mu(r) \to M_+, \quad \phi(r) \to 0, \quad \text{as } r \to \infty. \tag{3.7}$$

If we expand eqs. (3.3)–(3.5) about the horizon, we obtain a relation between $\phi'(r_h)$ and $\phi(r_h)$ which fixes an additional boundary condition,

$$\phi'(r_h) = \frac{r_h V_\phi[\phi(r_h)]}{1 - 8\pi G r_h^2 V[\phi(r_h)]}. \tag{3.8}$$

This is analogous to the condition $\phi'(0) = 0$ in the $O(4)$ case. The boundary value problem appears to be overdetermined, but this is simply because the remnant mass parameter μ_- is determined by the value of the seed mass M_+. In practise, we solve the system of equations using a shooting method, integrating from the horizon for a given μ_- and trying different initial values of $\phi(r_h)$. The integration leads to an asymptotic value for the seed mass M_+ for a given remnant mass parameter. From this we can infer the remnant mass for a given seed mass.

Before presenting some sample solutions, it is useful to first discuss what we expect for our functions, using the thin-wall static instantons as a model solution. Note that

JHEP06(2016)025

the variable $\mu(r)$ includes reference to the negative cosmological constant on the true vacuum side:

$$\mu_{\text{thin}}(r) = \begin{cases} M_- - r^3/2G\ell^2 & r < r_+ \\ M_+ & r \geq r_+ \end{cases} \tag{3.9}$$

where ℓ is the AdS curvature radius. Meanwhile, $\phi(r)$ makes a sharp transition from false to true vacuum at the static instanton bubble radius, r_+. As we move away from the thin wall limit, we might expect ϕ to be close to its true vacuum value to some distance outside the horizon before making a more (or less) sharp transition to the false vacuum at large r, the exception to this behaviour being when $\lambda_6 = 0$, in which case there is no new minimum, and the field will simply roll immediately from its maximal value at the horizon to the minimum at large r. Since $\mu(r)$ responds to the energy-momentum tensor, we would expect that as the wall thickens, the sharp jump in $\mu(r)$ at r_+ will be rounded off and spread out, with the function following the same broad shape, but smoothly. As the wall becomes thicker still, the effect of the cosmological constant (which makes μ negative) will become more muted, until for the über-thick wall ($\lambda_6 = 0$) the behaviour of μ will be dominated by the $\phi-$energy-momentum, and will be mostly positive.

Figure 6 shows the profiles of the ϕ and μ functions as the λ_6 parameter is switched on. For $\lambda_6 = 0$, there is no second minimum of the potential which simply rolls to larger negative values. We expect therefore that the scalar field will start to roll away from its horizon value immediately, and the black hole to have a scalar 'cloak' where the field is rapidly falling to the false vacuum. The μ profile correspondingly is mostly positive, with just a small dip near the horizon where the larger negative potential has an impact. As λ_6 is switched on, the 'domain wall' nature of the $\phi-$profile begins to show. In figure 6 an intermediate value of λ_6 is shown, where the field stays near the true vacuum in the vicinity of the horizon, but then falls to the true vacuum over a reasonably thick range of r. The geometry function μ again starts with the cosmological constant dominated profile, before rising again as the energy-momentum of the wall causes the mass parameter to change. Finally the profiles are shown for λ_6 very close to the thin wall limit. Here, we see the $\phi-$profile stays approximately at the true vacuum for a large range of r near the horizon, then falls relatively rapidly to the false vacuum at large r. The $\mu-$profile tracks the exact Schwarzschild-AdS form until the scalar starts to fall, when it makes a rapid transition up to the asymptotic Schwarzschild form.

3.2 Computing the action and decay rates

The $O(3) \times \mathrm{U}(1)$ symmetry results in a simple formula for the tunnelling exponent B, derived in ref. [30]:

$$B = \frac{\mathcal{A}_+}{4G} - \frac{\mathcal{A}_-}{4G}, \tag{3.10}$$

where $\mathcal{A}_+$ is the horizon area of the seed black hole and $\mathcal{A}_-$ is the horizon area of the remnant back hole. The action can also be expressed in terms of the black hole mass parameters,

$$B = \frac{M_+^2 - \mu_-^2}{2M_p^2}. \tag{3.11}$$

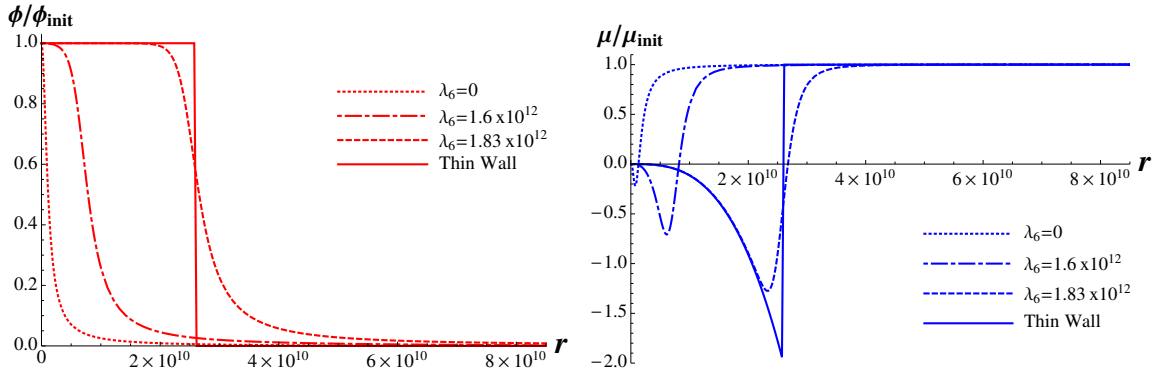

Figure 6. The solutions for μ and ϕ outside the event horizon. Relative profiles of ϕ and μ are shown, where ϕ is shown relative to its value at the horizon (the maximum) and the μ function relative to its asymptotic value, M_+.

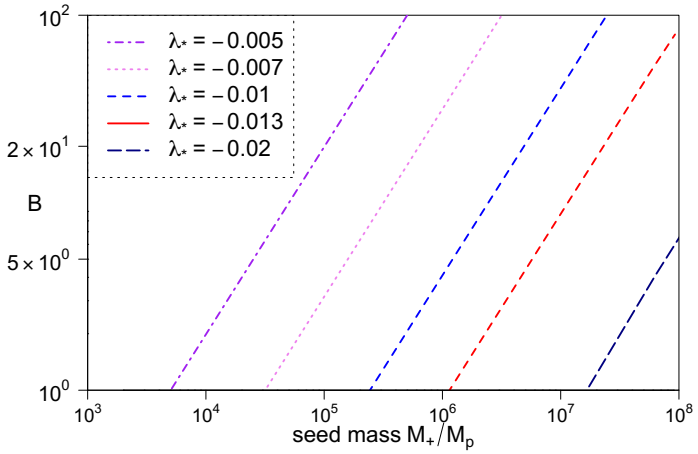

Figure 7. The action of the bounce solution is shown as a function of the seed mass for various values of λ_*.

We now see why choosing the parameter μ in the numerical integration is so convenient — the tunneling amplitude is simply expressed in terms of the initial and final values of μ. For a given scalar field potential V, we can obtain a range of data for different seed masses by integrating out from the horizon.

Results for the bounce action are shown for different values of the seed mass M_+ in figure 7. The vacuum decay formalism includes a condition that the action $B > 1$, and so the plots have been restricted to this range. The plot shows a range of values for the seed mass where the bounce action is far smaller than the action of the O(4) solutions shown in figure 3. Vacuum decay is enhanced by black holes in this mass range.

Given that the seed masses of the black holes favourably catalysing vacuum decay are rather small, the crucial feature we have to factor in is whether the vacuum decay is preferential to Hawking evaporation of the black hole. The vacuum decay rate Γ_D is given by

$$\Gamma_D = Ae^{-B}, \tag{3.12}$$

JHEP06(2016)025

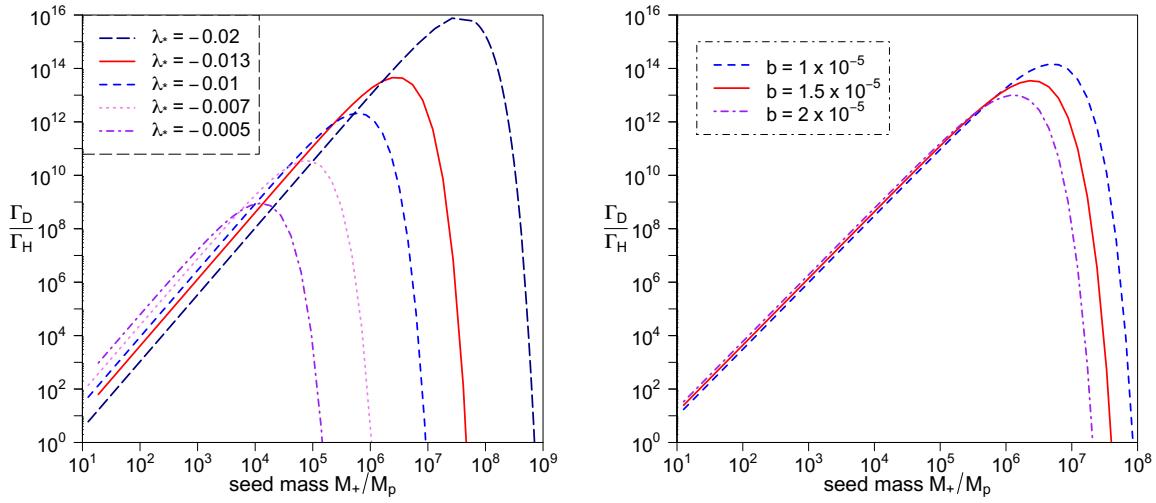

Figure 8. The branching ratio of the false vacuum nucleation rate to the Hawking evaporation rate is shown as a function of the seed mass for different values of the Higgs potential parameters λ_* (with $b = 1.4 \times 10^{-5}$) and b (with $\lambda_* = -0.013$).

where we have included the pre-factor A. This pre-factor is made up from a single factor of $(B/2\pi)^{1/2}$ for the translational zero mode of the instanton in the time direction, and a determinant factor. We use dimensional analysis to obtain a rough estimate $(GM_+)^{-1}$ for the determinant factor, yielding

$$\Gamma_D \approx \left(\frac{B}{2\pi}\right)^{1/2} (GM_+)^{-1} e^{-B}. \tag{3.13}$$

We may use the Hawking evaporation rate for a subset of the standard model evaluated by Page [43]. Setting $\Gamma_H = \dot{M}/M$, we have

$$\Gamma_H \approx 3.6 \times 10^{-4} (G^2 M_+^3)^{-1}\,. \tag{3.14}$$

Combining these results, we obtain the branching ratio of the tunnelling rate to the evaporation rate as

$$\frac{\Gamma_D}{\Gamma_H} \approx 43.8 \frac{M_+^2}{M_p^2} B^{1/2} e^{-B}. \tag{3.15}$$

This branching ratio has been plotted as a function of the seed mass M_+ for some sets of parameters in figure 8. A primordial black hole starting out with a mass around 10^{12} kg would decay by Hawking evaporation to the mass scales shown in figure 8 by the present day. At some point, the vacuum decay rate becomes larger than the Hawking evaporation rate and the black hole seeds vacuum decay. The vacuum decay dominates when the black hole mass is 10^5–10^9 times larger than the reduced Planck mass, depending on where the value of the top quark mass lies in the range 172–174GeV. The black holes are large enough for the semi-classical results to be valid, but with Hawking temperatures in the range 10^{13}–10^9 GeV their decay half-life is tiny, ranging from 10^{-24}–10^{-12} s.

The effect on the branching ratio of including a ϕ^6 term in the potential is shown in figure 9. The vacuum decay rate is reduced for positive values of λ_6. As the value of

JHEP06(2016)025

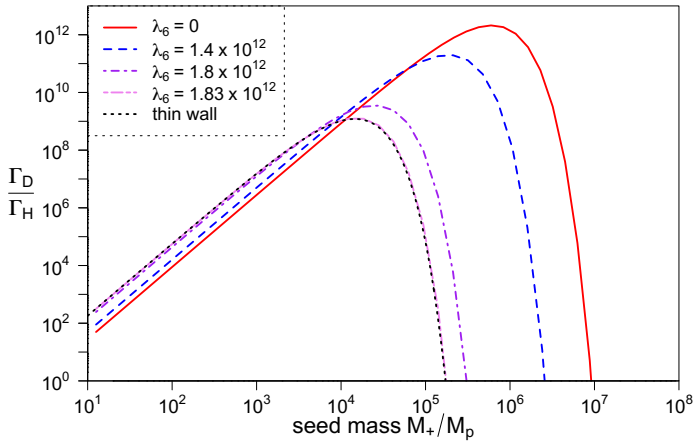

Figure 9. The branching ratio of the vacuum decay rate rate to the Hawking evaporation rate as a function of the seed mass with $\lambda_* = -0.01$ and different values of the λ_6 coefficient. Results using a thin-wall approximation are indistinguishable from the numerical results at the largest value of λ_6.

λ_6 is increased, the potential of the true vacuum rises and the bounce solution starts to resemble a region of true vacuum surrounded by a thin-wall transition to the false vacuum. This allows a cross-check of the numerical results by comparing the bounce action to the thin-wall results obtained analytically in ref. [27].

4 Discussion

We have shown that our previous result that black holes seed vacuum decay is extremely robust to the parameters of the Higgs potential. We used an analytic fit to the Higgs potential and explored a range of parameter space beyond that of the Standard Model. Whereas our previous results applied only to the nucleation of thin-wall bubbles and covered a very small region of parameter space, these new results apply for any bubble wall profile and show that black holes are very effective seeds for vacuum decay. Figure 10 shows the region of parameter space explored vs. the standard model parameter range.

The importance of these results lies in the fact that a single primordial black hole in the observable universe would cause the decay of the Standard Model Higgs vacuum, and therefore would contradict the Standard Model. Looking beyond the Standard Model, quantum gravity effects can suppress the vacuum decay rate by contributing ϕ^6 terms to the Higgs potential, but the vacuum decay rate still remains large unless the high-energy vacuum becomes the false vacuum, which happens when the coefficient λ_6 is around 10^{12}. A stable Higgs vacuum requires the new physics to change the barrier in the Higgs potential at energies around 10^{10}–10^{14}GeV.

Vacuum decay can also be enhanced if the λ_6 coefficient in the potential is negative. However, we have found that the Higgs field at the centre of the vacuum decay bubble lies very close to the Planck scale and the reliability of the effective potential becomes questionable for negative values of λ_6. For non-negative values of λ_6, vacuum decay rates

JHEP06(2016)025

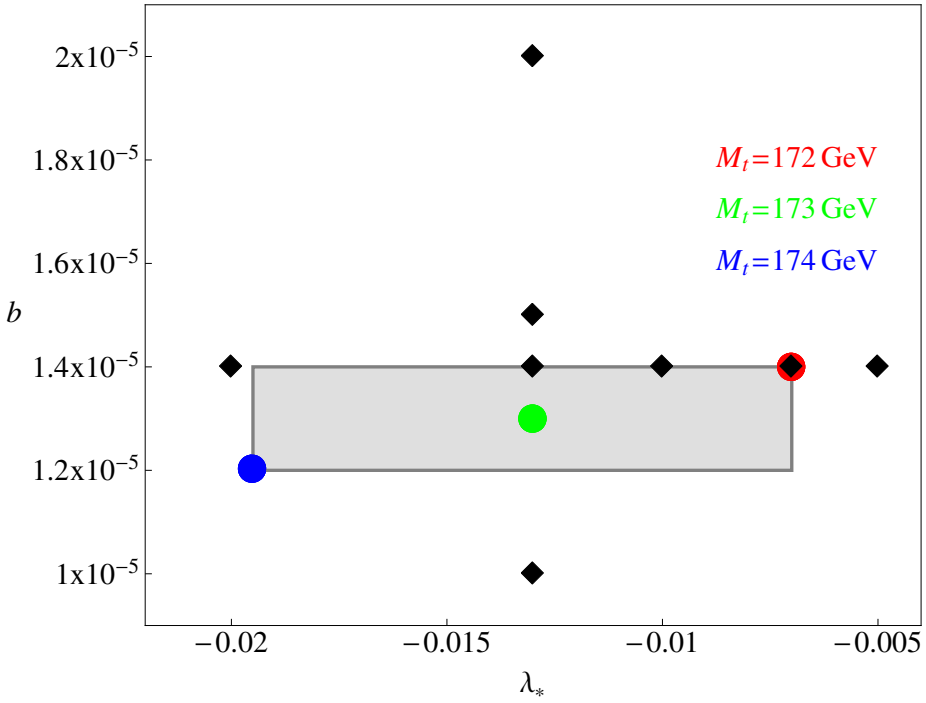

Figure 10. A representation of the parameter space we have explored numerically. The coloured plot markers represent the parameter values for the allowed range of top quark mass, 172–174GeV, and the diamond markers the specific parameter values we computed the branching ratio for in figure 8. The shaded box represents the parameter range covered by the Standard Model.

for unseeded vacuum decay bubbles are extremely small. Nevertheless, we have found a way to examine the evolution of the bubbles in real time and followed the interior towards a singularity.

Bubble nucleation in the presence of a black hole raises a number of questions which should be investigated further. The instanton approach, and its interpretation, are based on results which well understood in flat spacetimes but not rigorously described so far in the curved space context (although see [42, 44]). One question is the role of Hawking radiation in the tunnelling process. We have shown that the thermal evaporation rate is negligible, but there are still questions about the global spacetime structure, and why the result for the tunnelling rate is independent of the angle in the conical singularity arising in the instanton [27]. There is also a question about taking into account the way in which quantum corrections to the potential are affected by the spacetime curvature, although to some extent this question can be side-stepped by looking at black hole monopoles where the charge can be used to reduce the Hawking temperature, as was done in [30]. There are also a variety of interesting other consequences of finite temperature tunnelling, particularly in a cosmological context, see for example [45–47].

Besides primordial black holes, another source of nucleation seeds could be black holes formed by particle collisions in theories with a low fundamental Planck mass [48–52]. The possibility of vacuum decay caused by black holes formed from collisions was considered

JHEP06(2016)025

in [29, 30]. There is an observations constraint here due to long life of our vacuum state despite the existence of high energy cosmic ray collisions, which may place interesting limits on theories with a low fundamental Planck mass.

Finally, although we have considered bubbles inside a Schwarzschild (i.e. asymptotically flat) spacetime, AdS-AdS transitions, (such as considered in [53] to address the information problem) are obviously of interest. Static bubbles would now have the holographic interpretation of flows between field theories at different temperatures and different central charges. Flows and bubbles in AdS have of course already been considered, but the new aspect of having a black hole raises intriguing possibilities for thermal flows.

Acknowledgments

We would like to thank Erick Weinberg for useful discussions and Joan Elias-Miró for helpful correspondence. PB was supported in part by an EPSRC International Doctoral Scholarship, and by the Einstein Research Project "Gravitation and High Energy Physics", funded by the Einstein Foundation Berlin, the Israel Science Foundation grant no. 812/11 and by the Quantum Universe grant from the I-CORE program of the Israeli Planning and Budgeting Committee. RG and IGM are supported in part by STFC (Consolidated Grant ST/J000426/1). RG is also supported by the Wolfson Foundation and Royal Society, and Perimeter Institute for Theoretical Physics. Research at Perimeter Institute is supported by the Government of Canada through Industry Canada and by the Province of Ontario through the Ministry of Research and Innovation. RG would also like to thank the Aspen Center for Physics for hospitality. Work at Aspen is supported in part by National Science Foundation Grant No. PHYS-1066293 and the hospitality of the Aspen Center for Physics.

References

[1] S.R. Coleman, *The Fate of the False Vacuum. 1. Semiclassical Theory*, *Phys. Rev.* **D 15** (1977) 2929 [*Erratum ibid.* **D 16** (1977) 1248] [INSPIRE].

[2] C.G. Callan Jr. and S.R. Coleman, *The Fate of the False Vacuum. 2. First Quantum Corrections*, *Phys. Rev.* **D 16** (1977) 1762 [INSPIRE].

[3] S.R. Coleman and F. De Luccia, *Gravitational Effects on and of Vacuum Decay*, *Phys. Rev.* **D 21** (1980) 3305 [INSPIRE].

[4] I.Yu. Kobzarev, L.B. Okun and M.B. Voloshin, *Bubbles in Metastable Vacuum*, *Sov. J. Nucl. Phys.* **20** (1975) 644 [INSPIRE].

[5] G. Degrassi et al., *Higgs mass and vacuum stability in the Standard Model at NNLO*, *JHEP* **08** (2012) 098 [arXiv:1205.6497] [INSPIRE].

[6] D. Buttazzo et al., *Investigating the near-criticality of the Higgs boson*, *JHEP* **12** (2013) 089 [arXiv:1307.3536] [INSPIRE].

JHEP06(2016)025

[7] A. Gorsky, A. Mironov, A. Morozov and T.N. Tomaras, *Is the Standard Model saved asymptotically by conformal symmetry?*, *J. Exp. Theor. Phys.* **120** (2015) 344 [arXiv:1409.0492] [INSPIRE].

[8] F. Bezrukov and M. Shaposhnikov, *Why should we care about the top quark Yukawa coupling?*, *J. Exp. Theor. Phys.* **120** (2015) 335 [arXiv:1411.1923] [INSPIRE].

[9] J. Ellis, *Discrete Glimpses of the Physics Landscape after the Higgs Discovery*, *J. Phys. Conf. Ser.* **631** (2015) 012001 [arXiv:1501.05418] [INSPIRE].

[10] K. Blum, R.T. D'Agnolo and J. Fan, *Vacuum stability bounds on Higgs coupling deviations in the absence of new bosons*, *JHEP* **03** (2015) 166 [arXiv:1502.01045] [INSPIRE].

[11] G. Isidori, G. Ridolfi and A. Strumia, *On the metastability of the standard model vacuum*, *Nucl. Phys.* **B 609** (2001) 387 [hep-ph/0104016] [INSPIRE].

[12] M.S. Turner and F. Wilczek, *Is our vacuum metastable?*, *Nature* **298** (1982) 633 [INSPIRE].

[13] M. Lindner, M. Sher and H.W. Zaglauer, *Probing Vacuum Stability Bounds at the Fermilab Collider*, *Phys. Lett.* **B 228** (1989) 139 [INSPIRE].

[14] M. Sher, *Electroweak Higgs Potentials and Vacuum Stability*, *Phys. Rept.* **179** (1989) 273 [INSPIRE].

[15] I.V. Krive and A.D. Linde, *On the Vacuum Stability Problem in Gauge Theories*, *Nucl. Phys.* **B 117** (1976) 265 [INSPIRE].

[16] N. Cabibbo, L. Maiani, G. Parisi and R. Petronzio, *Bounds on the Fermions and Higgs Boson Masses in Grand Unified Theories*, *Nucl. Phys.* **B 158** (1979) 295 [INSPIRE].

[17] J.R. Espinosa, G.F. Giudice and A. Riotto, *Cosmological implications of the Higgs mass measurement*, *JCAP* **05** (2008) 002 [arXiv:0710.2484] [INSPIRE].

[18] G. Isidori, V.S. Rychkov, A. Strumia and N. Tetradis, *Gravitational corrections to standard model vacuum decay*, *Phys. Rev.* **D 77** (2008) 025034 [arXiv:0712.0242] [INSPIRE].

[19] J. Elias-Miro, J.R. Espinosa, G.F. Giudice, G. Isidori, A. Riotto and A. Strumia, *Higgs mass implications on the stability of the electroweak vacuum*, *Phys. Lett.* **B 709** (2012) 222 [arXiv:1112.3022] [INSPIRE].

[20] ATLAS collaboration, *Combined search for the Standard Model Higgs boson using up to 4.9 fb^{-1} of pp collision data at $\sqrt{s} = 7$ TeV with the ATLAS detector at the LHC*, *Phys. Lett.* **B 710** (2012) 49 [arXiv:1202.1408] [INSPIRE].

[21] CMS collaboration, *Combined results of searches for the standard model Higgs boson in pp collisions at $\sqrt{s} = 7$ TeV*, *Phys. Lett.* **B 710** (2012) 26 [arXiv:1202.1488] [INSPIRE].

[22] G.W. Gibbons and S.W. Hawking eds., *Euclidean quantum gravity*, World Scientific, Singapore (1993), pg. 586, ISBN: 981-02-0515-5.

[23] W. Israel, *Singular hypersurfaces and thin shells in general relativity*, *Nuovo Cim.* **B 44S10** (1966) 1 [*Erratum ibid.* **B 48** (1967) 463] [INSPIRE].

[24] W.A. Hiscock, *Can black holes nucleate vacuum phase transitions?*, *Phys. Rev.* **D 35** (1987) 1161 [INSPIRE].

[25] V.A. Berezin, V.A. Kuzmin and I.I. Tkachev, *$O(3)$ Invariant Tunneling in General Relativity*, *Phys. Lett.* **B 207** (1988) 397 [INSPIRE].

JHEP06(2016)025

[26] V.A. Berezin, V.A. Kuzmin and I.I. Tkachev, *Black holes initiate false vacuum decay*, *Phys. Rev.* **D 43** (1991) 3112 [INSPIRE].

[27] R. Gregory, I.G. Moss and B. Withers, *Black holes as bubble nucleation sites*, *JHEP* **03** (2014) 081 [arXiv:1401.0017] [INSPIRE].

[28] A. Aguirre and M.C. Johnson, *Dynamics and instability of false vacuum bubbles*, *Phys. Rev.* **D 72** (2005) 103525 [gr-qc/0508093] [INSPIRE].

[29] P. Burda, R. Gregory and I. Moss, *Gravity and the stability of the Higgs vacuum*, *Phys. Rev. Lett.* **115** (2015) 071303 [arXiv:1501.04937] [INSPIRE].

[30] P. Burda, R. Gregory and I. Moss, *Vacuum metastability with black holes*, *JHEP* **08** (2015) 114 [arXiv:1503.07331] [INSPIRE].

[31] V. Branchina and E. Messina, *Stability, Higgs Boson Mass and New Physics*, *Phys. Rev. Lett.* **111** (2013) 241801 [arXiv:1307.5193] [INSPIRE].

[32] V. Branchina, E. Messina and M. Sher, *Lifetime of the electroweak vacuum and sensitivity to Planck scale physics*, *Phys. Rev.* **D 91** (2015) 013003 [arXiv:1408.5302] [INSPIRE].

[33] C. Ford, D.R.T. Jones, P.W. Stephenson and M.B. Einhorn, *The effective potential and the renormalization group*, *Nucl. Phys.* **B 395** (1993) 17 [hep-lat/9210033] [INSPIRE].

[34] A. Shkerin and S. Sibiryakov, *On stability of electroweak vacuum during inflation*, *Phys. Lett.* **B 746** (2015) 257 [arXiv:1503.02586] [INSPIRE].

[35] K.G. Chetyrkin and M.F. Zoller, *Three-loop β-functions for top-Yukawa and the Higgs self-interaction in the Standard Model*, *JHEP* **06** (2012) 033 [arXiv:1205.2892] [INSPIRE].

[36] F. Bezrukov, M.Yu. Kalmykov, B.A. Kniehl and M. Shaposhnikov, *Higgs Boson Mass and New Physics*, *JHEP* **10** (2012) 140 [arXiv:1205.2893].

[37] C.P. Burgess, *Quantum gravity in everyday life: General relativity as an effective field theory*, *Living Rev. Rel.* **7** (2004) 5 [gr-qc/0311082] [INSPIRE].

[38] F. Loebbert and J. Plefka, *Quantum Gravitational Contributions to the Standard Model Effective Potential and Vacuum Stability*, *Mod. Phys. Lett.* **A 30** (2015) 1550189 [arXiv:1502.03093] [INSPIRE].

[39] Z. Lalak, M. Lewicki and P. Olszewski, *Higher-order scalar interactions and SM vacuum stability*, *JHEP* **05** (2014) 119 [arXiv:1402.3826] [INSPIRE].

[40] D. Garfinkle and R. Gregory, *Corrections to the Thin Wall Approximation in General Relativity*, *Phys. Rev.* **D 41** (1990) 1889 [INSPIRE].

[41] F. Bonjour, C. Charmousis and R. Gregory, *Thick domain wall universes*, *Class. Quant. Grav.* **16** (1999) 2427 [gr-qc/9902081] [INSPIRE].

[42] A.R. Brown and E.J. Weinberg, *Thermal derivation of the Coleman-De Luccia tunneling prescription*, *Phys. Rev.* **D 76** (2007) 064003 [arXiv:0706.1573] [INSPIRE].

[43] D.N. Page, *Particle Emission Rates from a Black Hole: Massless Particles from an Uncharged, Nonrotating Hole*, *Phys. Rev.* **D 13** (1976) 198 [INSPIRE].

[44] V.A. Rubakov and S.M. Sibiryakov, *False vacuum decay in de Sitter space-time*, *Theor. Math. Phys.* **120** (1999) 1194 [gr-qc/9905093] [INSPIRE].

[45] E. Greenwood, E. Halstead, R. Poltis and D. Stojkovic, *Dark energy, the electroweak vacua and collider phenomenology*, *Phys. Rev.* **D 79** (2009) 103003 [arXiv:0810.5343] [INSPIRE].

JHEP06(2016)025

[46] C. Cheung and S. Leichenauer, *Limits on New Physics from Black Holes*, *Phys. Rev.* **D 89** (2014) 104035 [arXiv:1309.0530] [INSPIRE].

[47] J.R. Espinosa et al., *The cosmological Higgstory of the vacuum instability*, *JHEP* **09** (2015) 174 [arXiv:1505.04825] [INSPIRE].

[48] N. Arkani-Hamed, S. Dimopoulos and G.R. Dvali, *The hierarchy problem and new dimensions at a millimeter*, *Phys. Lett.* **B 429** (1998) 263 [hep-ph/9803315] [INSPIRE].

[49] I. Antoniadis, N. Arkani-Hamed, S. Dimopoulos and G.R. Dvali, *New dimensions at a millimeter to a Fermi and superstrings at a TeV*, *Phys. Lett.* **B 436** (1998) 257 [hep-ph/9804398] [INSPIRE].

[50] L. Randall and R. Sundrum, *A large mass hierarchy from a small extra dimension*, *Phys. Rev. Lett.* **83** (1999) 3370 [hep-ph/9905221] [INSPIRE].

[51] P. Kanti, *Black holes in theories with large extra dimensions: A review*, *Int. J. Mod. Phys.* **A 19** (2004) 4899 [hep-ph/0402168] [INSPIRE].

[52] R. Gregory, *Braneworld black holes*, *Lect. Notes Phys.* **769** (2009) 259 [arXiv:0804.2595] [INSPIRE].

[53] M. Sasaki and D.-h. Yeom, *Thin-shell bubbles and information loss problem in anti de Sitter background*, *JHEP* **12** (2014) 155 [arXiv:1404.1565] [INSPIRE].

JHEP06(2016)025